Whole-exome sequencing identifies *USH2A* mutations in a pseudo-dominant Usher syndrome family

SUI-LIAN ZHENG[1,2*], HONG-LIANG ZHANG[3*], ZHEN-LANG LIN[2] and QIAN-YAN KANG[1]

[1]Department of Ophthalmology, The First Affiliated Hospital, Xi'an Jiaotong University School of Medicine, Xi'an, Shaanxi 710061; [2]The Second Affiliated Hospital and Yuying Children's Hospital, Wenzhou Medical University, Wenzhou, Zhejiang 325027; [3]Anyang Eye Hospital, Anyang, Henan 455000, P.R. China

Received January 30, 2015; Accepted August 17, 2015

DOI: 10.3892/ijmm.2015.2322

Abstract. Usher syndrome (USH) is an autosomal recessive (AR) multi-sensory degenerative disorder leading to deaf-blindness. USH is clinically subdivided into three subclasses, and 10 genes have been identified thus far. Clinical and genetic heterogeneities in USH make a precise diagnosis difficult. A dominant-like USH family in successive generations was identified, and the present study aimed to determine the genetic predisposition of this family. Whole-exome sequencing was performed in two affected patients and an unaffected relative. Systematic data were analyzed by bioinformatic analysis to remove the candidate mutations via step-wise filtering. Direct Sanger sequencing and co-segregation analysis were performed in the pedigree. One novel and two known mutations in the *USH2A* gene were identified, and were further confirmed by direct sequencing and co-segregation analysis. The affected mother carried compound mutations in the *USH2A* gene, while the unaffected father carried a heterozygous mutation. The present study demonstrates that whole-exome sequencing is a robust approach for the molecular diagnosis of disorders with high levels of genetic heterogeneity.

Introduction

Usher syndrome (USH) is an autosomal recessive (AR) inherited disease belonging to the group of retinitis pigmentosa (RP) syndromes and is a clinical and genetically heterogeneous disease (1,2). Patients with USH usually exhibit progressive visual loss, hearing impairment and vestibule dysfunction. Clinically, USH is subdivided into three subclasses based on the severity and progression of the hearing impairment and whether the vestibule invaded. Type 1 USH is the most severe form, with the prepubertal onset of progressive RP, profound hearing loss and vestibular dysfunction. Type 2 USH is the most common type and is less severe, with moderate to severe congenital deafness and later-onset RP, but with the absence of vestibular dysfunction. Type 3 is the least common type, with progressive deafness, adult-onset RP, hypermetropic astigmatism and a variable impairment of vestibular function. Currently, 10 genes that are associated with this disease have been identified, and three loci have been mapped in human chromosomes (http://www.retinogenetics.org).

Thus far, increasing attention has been paid to the molecular diagnosis of USH. The Sanger sequencing of the coding region, a traditional approach, is reliable and provides an easy strategy to determine the genetic causes of a disease (3). However, Sanger sequencing is not always affordable due to the large number of coding fragments. A USH genotyping microarray based on arrayed primer extension technology was used to simultaneously screen multiple known sites; however, it was unable to detect new mutations, insertions or deletions (Indels) (4,5). Custom-designed targeted exome sequencing is a high-throughput and cost-effective method that permits the screening of a number of previously targeted coding regions (6,7). To cover full coding regions in the human genome, whole-exome sequencing has been developed to facilitate the discovery of novel disease genes (8).

In the present study, a pseudo-dominant pedigree of USH was identified, which presented as dominant heritance, in patients over two successive generations. As all of the known genes are a recessive trait, we speculated that a novel causative gene in the dominant pattern was mutated in this family. To determine the genetic predisposition, whole-exome sequencing was applied and one novel and two known *USH2A* mutations were identified that successfully explained the genetic architecture in this family.

Materials and methods

Subject recruitment. The study was carried out in adherence to the tenets of the Declaration of Helsinki and was approved by the Ethics Committee of the Eye Hospital of Wenzhou Medical University (Wenzhou, Zhejiang, China). All the study subjects

Correspondence to: Professor Qian-Yan Kang, Department of Ophthalmology, The First Affiliated Hospital, Xi'an Jiaotong University School of Medicine, 277 West Yanta Road, Xi'an, Shaanxi 710061, P.R. China
E-mail: kangqy@mail.xjtu.edu.cn; qianyankang@163.com

*Contributed equally

Key words: whole-exome sequencing, Usher syndrome, *USH2A* gene mutation

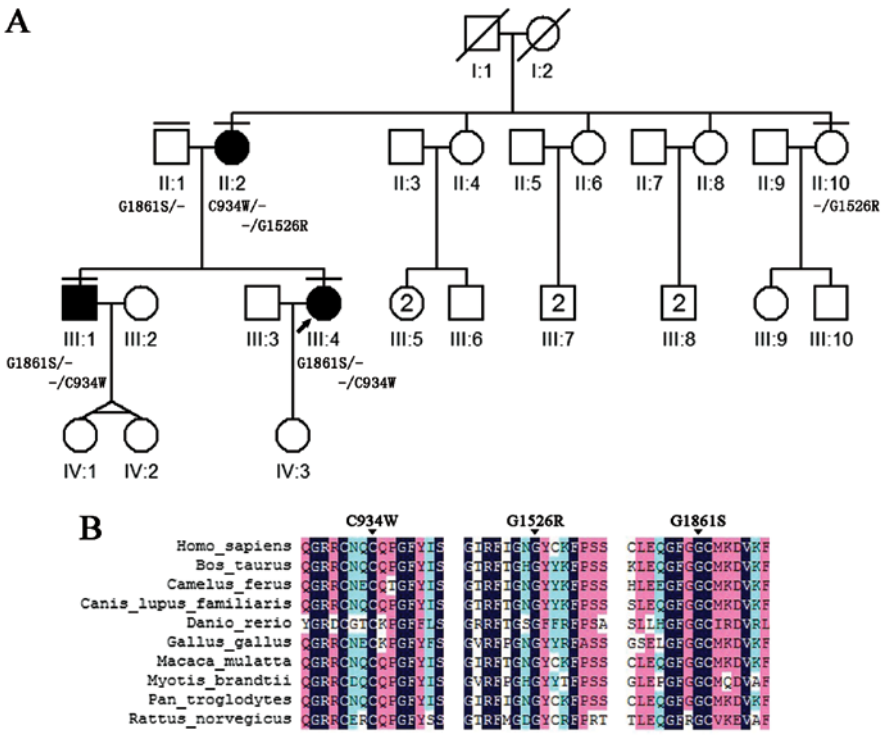

Figure 1. Pedigree and conservation of mutations in the Usher syndrome type IIA (*USH2A*) gene. (A) Three mutations were identified in a family with Usher syndrome. (B) All the missense mutations in the *USH2A* gene were located within a region that is highly conserved among different species.

were fully informed, and consent was obtained. In the study, five individuals, including two males and three females, from a Chinese family exhibited phenotypic features that were consistent with USH and a pseudo-dominant inheritance pattern from the Division of Ophthalmic Genetics at the Eye Hospital of Wenzhou Medical University. The clinical diagnosis of USH was based on typical visual loss due to RP and progressive hearing impairment. Comprehensive ophthalmic tests were performed on each patient, including tests of visual acuity, fundus photography, optical coherence tomography, electroretinography (ERG) and perimetry. The primary complaints from patients were night blindness, visual field restriction and hearing loss, in addition to typical symptoms, including bone spicule-like pigmentation, retinal vessel attenuation and waxy disc pallor in the fundus. A more detailed family history was obtained via personal interviews with the patients and family members (Fig. 1). Peripheral blood samples were collected following informed consent from all five of the subjects. Three genomic DNA samples, including samples from two affected individuals (II:2 and III:1) and one unaffected individual (II:1), were selected for whole-exome sequencing, and two samples from affected individuals (III:4 and II:10) were tested for mutation validation using Sanger sequencing.

DNA preparation. Genomic DNA was extracted from leukocytes using the TIANamp Blood DNA kit (Tiangen, Beijing, China) according to the manufacturer's instructions. The DNA concentration was quantified using a spectrophotometer (NanoDrop 1000; Thermo Fisher Scientific, Waltham, MA, USA).

Whole-exome sequencing. The library was prepared and the exome was captured using the Illumina HiSeq 2000 platform based on the manufacturer's instructions (9). In brief, a minimum of 3 μg genomic DNA was sheared, end-repaired and ligated with special devices. The genomic DNA of each subject was sheared into fragments ranging from 350-400 base pairs. Following adaptor ligation, the library was amplified according to standard Illumina protocols, and the polymerase chain reaction (PCR) product was validated using the Agilent Bioanalyzer (Santa Clara, CA, USA). Capture enrichment was performed by twice hybridization and washing using specially designed capture probes and streptavidin beads; subsequently, the exome-targeted DNA library was enriched. In short, PCR was used to amplify the enriched library, as in the previous step. Subsequent to the final product being amplified and validated, the library was enriched for sequencing on the Illumina HiSeq 2000 sequencer.

Sequencing data analysis. Following sequencing on the Illumina HiSeq 2000 platform, the primary data were processed to retrieve high-quality reads using the SolexaQA package and the cutadapt program (http://code.google.com/p/cutadapt/). The clean sequence reads were aligned to the reference human genome (hg19) using the SOAPaligner program. Subsequently, the dataset files, including the PCR duplicates that were removed and the identified SNPs, were analyzed using the Picard software and SOAPsnp program, respectively. Variants of the Indels were identified using the GATK program. All the identified variants were annotated by the exome-assistant program (10). In addition, the variants with a frequency >1% were removed and the SIFT (http://sift.jcvi.org/www/SIFT_enst_submit.html), PolyPhen (http://genetics.bwh.harvard.edu/pph2/) and MutationTaster (http://www.mutationtaster.org/) programs were used to predict the effects of the variants on the protein function. As the pedigree in the study

Table I. Clinical phenotype of the patients in the pedigree.

Subjects	Gender	Age, years	Age at onset of blindness	RP	Age at onset of deafness	Vestibular dysfunction	Astigmatism	BCVA, R/L
II:2	F	51	<5 years	+	20 years	-	+	0.3/0.4
III:1	M	33	15 years	+	28 years	+	+	0.5/0.7
III:4	F	29	20 years	+	-	-	+	0.7/0.9

M, male; F, female; BCVA, best corrected visual acuity; RP, retinitis pigmentosa; R, right eye; L, left eye.

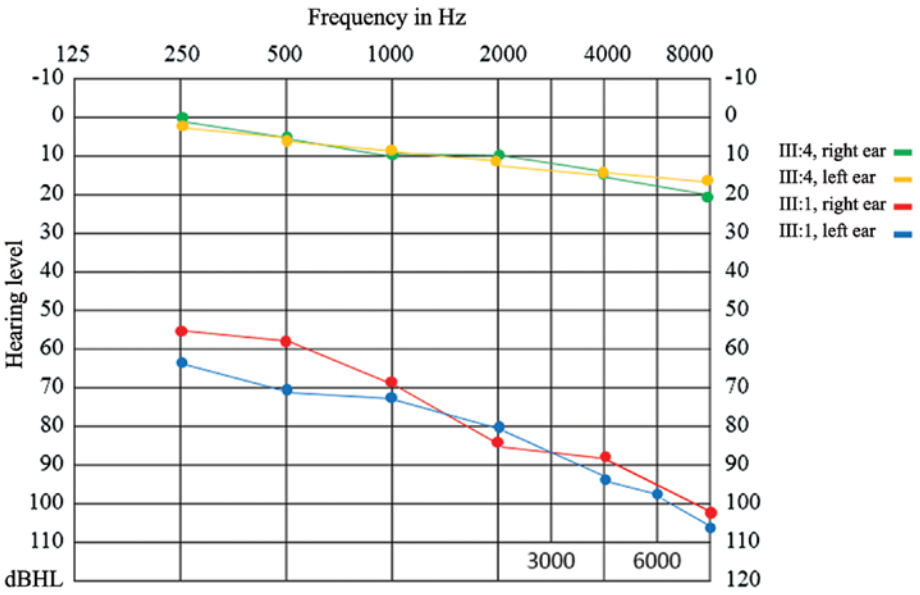

Figure 2. Audiogram test. Audiogram test showed bilateral downward-sloping moderate hearing loss in patient III:1, and patient III:4 exhibited normal audiogram function.

exhibited 'autosomal dominant' transmission, the candidate variants that were located in the dominant inherited alleles were first analyzed; however, no positive result was obtained; subsequently, the recessive inherited variants in the data were fully analyzed from the three whole-exome sequencing runs and the candidate mutations were identified.

Candidate mutation confirmation by Sanger sequencing. The candidate mutations were listed following the above standard filtering strategy in the whole-exome sequencing data of the three subjects. The specific primers were designed using Primer3 to amplify each coding region of the potential mutation. Following amplification by PCR, the products were sequenced by Sanger sequencing to further validate the precision of the candidate mutations. The Sanger sequencing data were analyzed by Mutation Surveyor (SoftGenetics, State College, PA, USA).

Results

Clinical phenotype. In order to clinically characterize the patients, a detailed family history was obtained and full ophthalmology examinations were performed on all the patients. Night blindness and peripheral visual field constriction were reported by every patient. Two patients (II:2 and III:1) were characterized by moderate progressive hearing loss with the onset of their second decade, and one of these patients (III:1) exhibited impaired vestibular function (Table I). Audiogram showed bilateral downward-sloping moderate hearing loss in patient III:1, while patient III:4 exhibited normal audiogram function (Fig. 2). Fundus photography revealed typical RP signs, including mottling and granularity of the RPE, attenuated retinal vessels and optic nerve head pallor, in every patient (II:2, III:1 and III:4). The ERG results clearly showed profound abnormalities with no detectable rod response (Fig. 3). The static visual field (Humphrey Field Analyzer 24-2) exhibited a greater decrease in the retinal sensitivity in the far periphery. Color vision defects and astigmatism were found in all the affected patients. All the symptoms, particularly those typical of RP and progressive deafness, in this pedigree supported a diagnosis of USH. However, based on the clinical symptoms that were aforementioned, it is difficult to diagnose which subtype of USH this family belongs to. In addition, the inheritance pattern of USH has only been reported as AR transmission; therefore, it was suggested this pedigree is caused by a novel dominant gene.

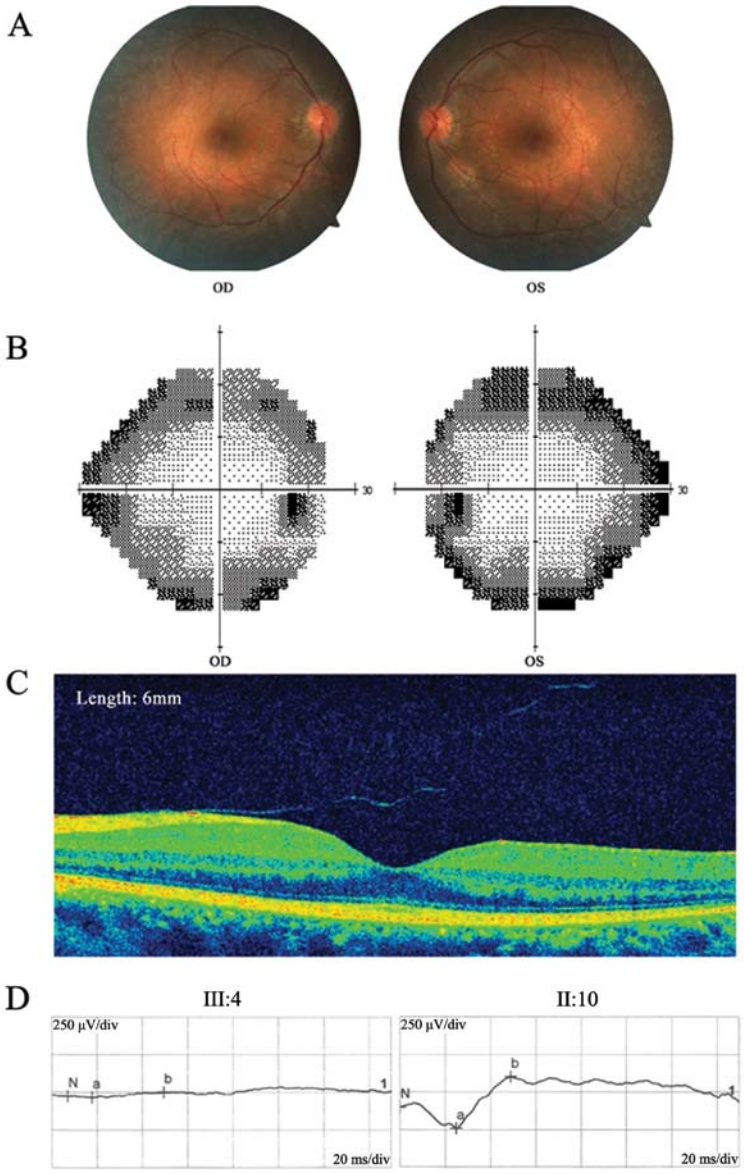

Figure 3. Clinical observations. (A) A fundoscopy of the proband patient (III:4) presented extensive degeneration in both eyes. (B) The visual field constriction (III:4). (C) The optical coherence tomography indicated that the retinal thickness was decreased (III:4). (D) The electroretinography showed an extinguished response in a patient (III:4) and a normal response in the healthy relative (II:10).

Identification of candidate mutations by whole-exome sequencing. Three subjects, including two affected individuals (II:2 and III:1) and one unaffected individual (II:1), in the pedigree were sequenced by whole-exome sequencing using the Illumina HiSeq 2000 platform. From the whole-exome sequencing, the average read depth of the targeted regions and the distribution of the sequencing depth indicated a high sequencing quality (Table II and Fig. 4). Combining the pedigree clinical phenotype and pathogenic genomic transmission mode, the candidate mutations were finally identified. Through the aforementioned filtering strategy, three candidate mutations were identified for this pedigree.

Mutation validation. The consistency of the Sanger sequencing results confirmed all the mutations in the three subjects (II:1, II:2 and III:1). Notably, the family showed a genetic continuity that appeared to be a dominant inherited pedigree; one heterozygous *USH2A* mutation (G1861S) was identified in the unaffected father (II:1), two compound heterozygous *USH2A* mutations (C934W and G1526R) in the affected mother (II:2) and two compound heterozygous *USH2A* mutations (C934W and G1861S) in the affected son (III:1) (Figs. 1 and 5; Table III). The validated results of the pedigree indicate that the affected son (II:1) inherited one heterozygous mutation (G1861S) from the father (II:1) and another (C934W) from the mother (II:2), which contributed to the illness. To further confirm these results, the familial validation was expanded in the affected daughter (III:4). Via a traditional direct sequencing of III:4, two compound heterozygous mutations (C934W and G1861S) in the *USH2A* gene were successfully identified. All the mutations of C934W and G1526R were confirmed in the mother (II:2), who was an affected patient; however, only C934W was transmitted to the two affected children (III:1 and III:4). The healthy individual carried a heterozygous mutation (G1526R).

Table II. Result of exome sequencing data analysis.

Data analysis	Patient II:1	Patient II:2	Patient III:1
Total reads	67,379,716	55,680,718	72,086,038
Total yield, bp	6,805,351,316	5,623,752,518	7,280,689,838
Read length, bp	101.0	101.0	101.0
Target regions, bp	62,085,286	62,085,286	62,085,286
Average throughput depth of target regions	109.6X	90.6X	117.3X
Mappable reads (reads mapped to human genome)	50,349,216	41,366,342	54,726,489
Mappable yield, bp	4,933,335,174	4,051,988,166	5,371,273,701
% Mappable reads	74.7	74.3	75.9
% Coverage of target regions (>1X)	94.7	94.9	94.6
Number of on-target genotypes (>1X)	58,780,409	58,910,095	58,744,961
% Coverage of target regions (>10X)	87.8	82.6	87.5
Number of on-target genotypes (>10X)	54,531,850	51,291,897	54,349,898
Median read depth of target regions	46.0X	32.0X	50.0X
Mean read depth of target regions	46.8X	34.8X	52.0X

bp, base pair.

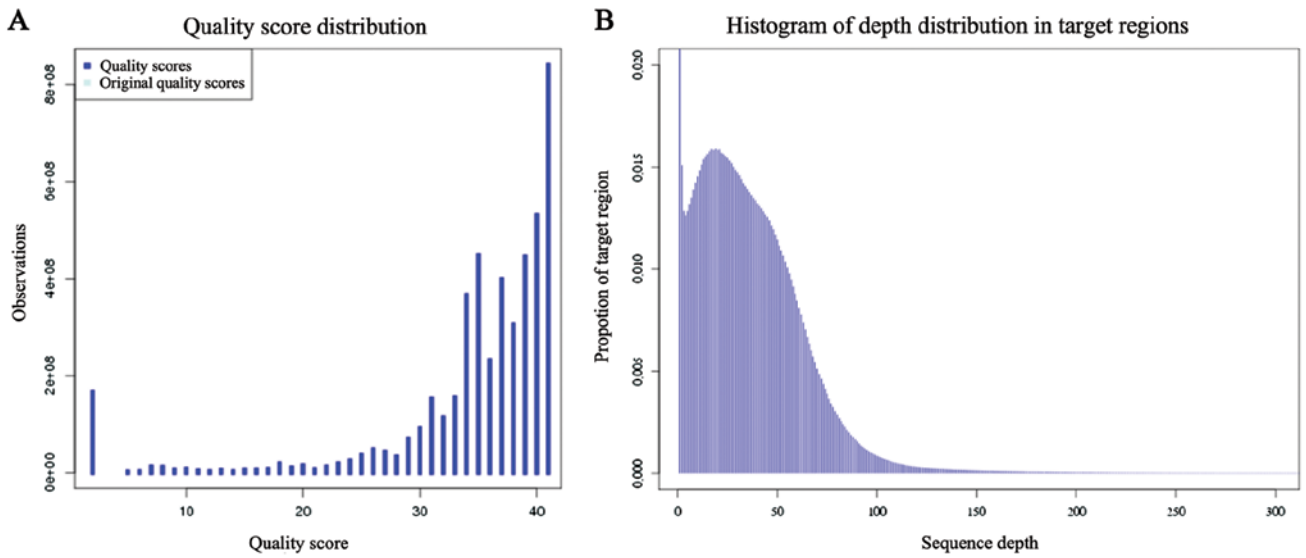

Figure 4. Whole-exome sequencing quality. (A) The quality score distribution. (B) The depth distribution in the target regions.

All these mutations were absent in 200 healthy controls. Taken together, the candidate mutations were validated using Sanger sequencing and a co-segregation trial.

Assessment of the pathogenicity of the mutations. In the study, one novel and two known *USH2A* gene mutations were identified in the pedigree and resulted in single amino acid substitutions at protein positions 934, 1526 and 1861 (p.C934W, p.G1526R and p.G1861S). To predict whether these amino acid changes were pathological, the combined evaluation of different computer algorithms, including SIFT, PolyPhen and MutationTaster (Table III), were used. The novel missense mutations were predicted to be deleterious. As all the missense mutations were also located in the highly phylogenetically conserved regions (Fig. 1), it was strongly suggested that the mutations in the *USH2A* gene were disease-causing and contributed to the disorder in this pedigree.

Discussion

USH is a monogenic disorder with AR inheritance. The worldwide prevalence of USH is relatively high, accounting for >50% of patients who are both deaf and blind (11,12). Visual acuity loss due to typical RP, congenital hearing impairment and variable vestibular dysfunction are the primary clinical symptoms. Based on these characteristics, USH could be divided clinically into three subtypes. USH is also a genetically heterogeneous disorder, and currently, 10 causative genes

Table III. Identified mutations in the pedigree.

Subject	Affected	Mutation	Type	Amino acid	Reported	SIFT	PolyPhen-2	MutationTaster
II:1	-	c.5581G>A	Hetero	G1861S	Reported	Damaging	Probably damaging	Disease causing
II:2	+	c.2802T>G	Hetero	C934W	Reported	Damaging	Probably damaging	Disease causing
		c.4576G>A	Hetero	G1526R	Novel	Tolerated	Probably damaging	Disease causing
II:10	-	c.4576G>A	Hetero	G1526R	Novel	Tolerated	Probably damaging	Disease causing
III:1	+	c.2802T>G	Hetero	C934W	Reported	Damaging	Probably damaging	Disease causing
		c.5581G>A	Hetero	G1861S	Reported	Damaging	Probably damaging	Disease causing
III:4	+	c.2802T>G	Hetero	C934W	Reported	Damaging	Probably damaging	Disease causing
		c.5581G>A	Hetero	G1861S	Reported	Damaging	Probably damaging	Disease causing

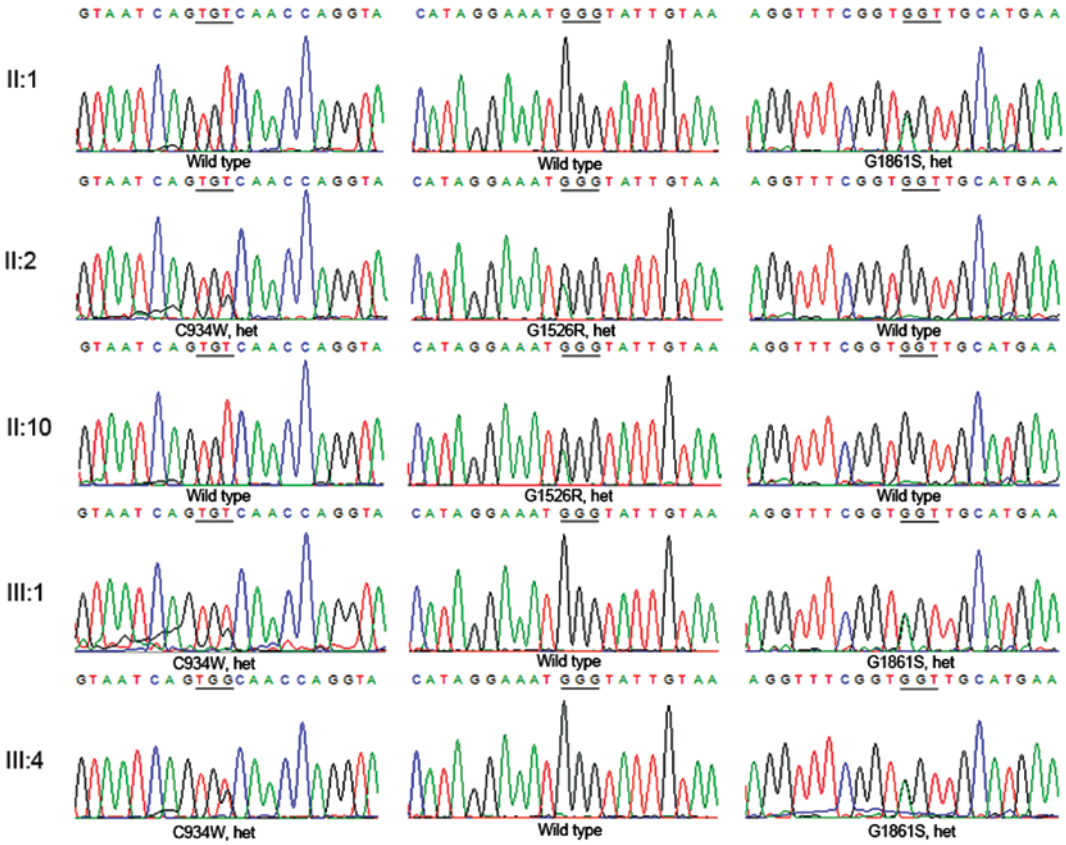

Figure 5. Identification of mutations in the *USH2A* gene. The sequence chromatograms were identified in five individuals.

have been identified. In addition, 3 loci (USH1E, USH1H and USH1K) have been mapped. Type 1 USH is caused by mutations in *MYO7A*, *USH1C*, *USH1G*, *CDH23*, *PCDH15* and *CIB2*; type 2 USH is caused by mutations in *USH2A*, *DFNB31* and *GPR98*; and type 3 USH is caused by mutations in *CLRN1*. However, the correlations between the phenotype and genotype are highly complex (13,14). Among these correlations, *USH2A* and *CLRN1* were reported in AR RP; and *CDH23*, *CIB2*, *DFNB31*, *MYO7A*, *PCDH15* and *USH1C* were identified in AR deafness alone or as a syndrome. In the present pedigree, five individuals, including three affected and two unaffected, were studied. Although RP, the primary symptom of USH, was described in three of the patients, the phenotype of each affected individual was distinct. The mother (II:2), who was a patient, suffered from RP and progressive deafness but no vestibular dysfunction, and the affected son (III:1) suffered from RP, progressive deafness and vestibular dysfunction. Notably, the affected daughter (III:4) suffered from RP without deafness and vestibular dysfunction, despite carrying the same genotype as that of the affected son (III:1). From the characteristics of USH that are aforementioned, it was suggested that different mutations in one gene could cause different phenotypes, and that the same mutations could cause intrafamilial phenotypic variability.

Taken together with the fact that more than a dozen genes contribute to USH, Sanger sequencing is not a good method for screening all the coding exons of all the causative genes due to its huge workload and low efficiency. As the appearance

of next-generation sequencing, whole-exome sequencing has proven to be an efficient diagnostic method for disorders with high degrees of genetic heterogeneity. Whole-exome sequencing can sequence coding regions of genomic DNA and can optimally screen huge number of genes, particularly disease-causing loci. Three subjects were selected, including two affected patients and one healthy relative, to undergo exome sequencing. Through data analysis and Sanger sequencing confirmation, one heterozygous mutation in the healthy father, two compound heterozygous mutations in the affected mother and two compound heterozygous mutations in the affected son were quickly identified. By Sanger sequencing, two compound heterozygous mutations were reconfirmed in the affected daughter (III:4) that were the same as those in the affected son (III:1). From the above results, it was revealed that the father is a carrier who transmitted the defective allele to his children and that the mother transmitted C934W to her children. This pedigree illustrates a pseudo-dominant family. Considering a previous study of *USH2A* mutations causing pseudo-dominant USH (6), it is possible that the carrier of the *USH2A* mutation is relatively common in the Chinese population. Thus, it may be a priority to screen *USH2A* when a pseudo-dominant USH family is diagnosed. Taken together, the present study successfully identified the *USH2A* mutations in the family using whole-exome sequencing and demonstrated the robustness of whole-exome sequencing to precisely diagnose USH.

In conclusion, one novel and two known *USH2A* mutations were identified using whole-exome sequencing in a pseudo-dominant USH family. These results highlight the possibility that the *USH2A* gene has an important role in Chinese pseudo-dominant USH and that whole-exome sequencing is a valuable approach for the genomic diagnosis of disorders with high degrees of genomic heterogeneity.

Acknowledgements

The authors gratefully acknowledge all the participants in the study.

References

1. Licastro D, Mutarelli M, Peluso I, Neveling K, Wieskamp N, Rispoli R, Vozzi D, Athanasakis E, D'Eustacchio A, Pizzo M, *et al*: Molecular diagnosis of Usher syndrome: Application of two different next generation sequencing-based procedures. PLoS One 7: e43799, 2012.
2. Millán JM, Aller E, Jaijo T, Blanco-Kelly F, Gimenez-Pardo A and Ayuso C: An update on the genetics of usher syndrome. J Ophthalmol 2011: 417217, 2011.
3. Bonnet C, Grati M, Marlin S, Levilliers J, Hardelin JP, Parodi M, Niasme-Grare M, Zelenika D, Délépine M, Feldmann D, *et al*: Complete exon sequencing of all known Usher syndrome genes greatly improves molecular diagnosis. Orphanet J Rare Dis 6: 21, 2011.
4. Vozzi D, Aaspõllu A, Athanasakis E, Berto A, Fabretto A, Licastro D, Külm M, Testa F, Trevisi P, Vahter M, *et al*: Molecular epidemiology of Usher syndrome in Italy. Mol Vis 17: 1662-1668, 2011.
5. Jaijo T, Aller E, García-García G, Aparisi MJ, Bernal S, Avila-Fernández A, Barragán I, Baiget M, Ayuso C, Antiñolo G, *et al*: Microarray-based mutation analysis of 183 Spanish families with Usher syndrome. Invest Ophthalmol Vis Sci 51: 1311-1317, 2010.
6. Huang XF, Xiang P, Chen J, Xing DJ, Huang N, Min Q, Gu F, Tong Y, Pang CP, Qu J, *et al*: Targeted exome sequencing identified novel USH2A mutations in Usher syndrome families. PLoS One 8: e63832, 2013.
7. Xing DJ, Zhang HX, Huang N, Wu KC, Huang XF, Huang F, Tong Y, Pang CP, Qu J and Jin ZB: Comprehensive molecular diagnosis of Bardet-Biedl syndrome by high-throughput targeted exome sequencing. PLoS One 9: e90599, 2014.
8. Jin ZB, Huang XF, Lv JN, Xiang L, Li DQ, Chen J, Huang C, Wu J, Lu F and Qu J: SLC7A14 linked to autosomal recessive retinitis pigmentosa. Nat Commun 5: 3517, 2014.
9. Soler VJ, Tran-Viet KN, Galiacy SD, Limviphuvadh V, Klemm TP, St Germain E, Fournié PR, Guillaud C, Maurer-Stroh S, Hawthorne F, *et al*: Whole exome sequencing identifies a mutation for a novel form of corneal intraepithelial dyskeratosis. J Med Genet 50: 246-254, 2013.
10. Liu Q, Shen E, Min Q, Li X, Wang X, Li X, Sun ZS and Wu J: Exome-assistant: A rapid and easy detection of disease-related genes and genetic variations from exome sequencing. BMC Genomics 13: 692, 2012.
11. Vernon M: Sociological and psychological factors associated with hearing loss. J Speech Hear Res 12: 541-563, 1969.
12. Boughman JA, Vernon M and Shaver KA: Usher syndrome: Definition and estimate of prevalence from two high-risk populations. J Chronic Dis 36: 595-603, 1983.
13. Méndez-Vidal C, González-Del Pozo M, Vela-Boza A, Santoyo-López J, López-Domingo FJ, Vázquez-Marouschek C, Dopazo J, Borrego S and Antiñolo G: Whole-exome sequencing identifies novel compound heterozygous mutations in USH2A in Spanish patients with autosomal recessive retinitis pigmentosa. Mol Vis 19: 2187-2195, 2013.
14. Besnard T, Vaché C, Baux D, Larrieu L, Abadie C, Blanchet C, Odent S, Blanchet P, Calvas P, Hamel C, *et al*: Non-USH2A mutations in USH2 patients. Hum Mutat 33: 504-510, 2012.